Canadian Mineralogist
Vol. 26, pp. 67-79 (1988)

PETROGENESIS AND CONDITIONS OF CRYSTALLIZATION OF SPANISH LAMPROITIC ROCKS

GIANPIERO VENTURELLI AND EMMA SALVIOLI MARIANI
Istituto di Petrografia, Università di Parma, 43100 Parma, Italy

STEPHEN F. FOLEY
Max Planck Institut für Chemie, Abt. Kosmochemie, 6500 Mainz, West Germany

SILVIO CAPEDRI
Istituto di Mineralogia e Petrologia, Università di Modena, 41100 Modena, Italy

ANTONY J. CRAWFORD
Department of Geology, University of Tasmania, Hobart, Tasmania, Australia

ABSTRACT

The lamproitic rocks of southeast Spain (8.6–6 Ma) occur mainly as dykes and plugs in the provinces of Murcia, Almeria and Albacete. Phlogopite, olivine, apatite, spinel, sanidine and glass are ubiquitous. Clinopyroxene, orthopyroxene, K-rich amphibole, biotite, ilmenite, pseudobrookite, leucite, analcime and carbonates may be additional phases. The magmas crystallized at temperatures below *ca.* 1200°C. Oxygen fugacity during crystallization varied from *ca.* WM at Calasparra to values intermediate between $Mn_{1-x}O$ - Mn_3O_4 (MnH in the text) and NNO at Jumilla and Aljorra. The $f(HF)/f(H_2O)$ and $f(HCl)/f(H_2O)$ ratios were very low (*ca.* 10^{-5} - 10^{-4}). The distribution of high-valency (>3) elements was largely influenced by the heterogeneous distribution of accessory phases in the source and by the melt structure. In particular, the $O/(Si+Ti+Al+Fe^{3+})$ ratio and P_2O_5 are well correlated, suggesting that the melts were saturated in apatite. The magmas were generated from an enriched mantle source containing phlogopite, orthopyroxene, olivine and accessory phases (*e.g.*, apatite). The source, however, before metasomatism, probably underwent loss of a magmatic component as suggested by the low contents of Ca, Na, Al and Sc.

Keywords: lamproites, southeast Spain, mineral chemistry, petrology.

SOMMAIRE

Les roches lamproïtiques du sud-est de l'Espagne (provinces de Murcia, Almeria et Albacete) se présentent surtout sous forme de dykes et de petites massifs. Phlogopite, olivine, apatite, spinelle, sanidine et verre sont très répandus. On rencontre aussi clinopyroxène, orthopyroxène, amphibole potassique, biotite, ilménite, pseudobrookite magnésienne, leucite, analcime et des carbonates. Les magmas ont cristallisé à une température inférieure à environ 1200°C. La fugacité d'oxygène était plutôt variable pendant la cristallisation, près du tampon WM à Calasparra et intermédiaire entre les tampons $Mn_{1-x}O$ - Mn_3O_4 (MnH dans le texte) et NNO à Jumilla et Aljorra. Les rapports $f(HF)/f(H_2O)$ et $f(HCl)/f(H_2O)$ étaient très bas (environ 10^{-5} - 10^{-4}). La distribution des éléments à valence élevée (>3) a été influencée par la distribution hétérogène des phases accessoires à la source et par la structure du magma. En particulier, le rapport $O/(Si+Ti+Al+Fe^{3+})$ et P_2O_5 montrent une bonne corrélation, qui fait penser que les magmas étaient saturés en apatite. Ces magmas ont pris naissance dans une région du manteau enrichie par métasomatisme et porteuse de phlogopite, orthopyroxène, olivine et phases accessoires, dont l'apatite. Avant le métasomatisme, par contre, la région aurait perdu une composante magmatique, comme l'indiquent les faibles teneurs en Ca, Na, Al et Sc.

(Traduit par la Rédaction)

Mots-clés: lamproïtes, Espagne, chimisme des minéraux, pétrologie.

INTRODUCTION

The ultrapotassic rocks of lamproitic character [Group 1 in Foley *et al.* (1987)] of southeastern Spain are distributed over a wide area (provinces of Murcia, Almeria and Albacete; Fig. 1) mainly in the form of plugs and dykes. They range from 8.6 to 5.5(?) Ma in age (Nobel *et al.* 1981, Bellon *et al.* 1983) and belong to the Na-poor Neogene magmatic province of southeastern Spain. Igneous suites of this province (Lopez Ruiz & Rodriguez Badiola 1980, Puga 1980) consist mainly of calcalkaline and shoshonitic volcanic rocks; lamproites are volumetrically scarce.

The Spanish lamproites show the following features: (i) magmatic plagioclase is typically absent; (ii) silica normally exceeds 53%, except for some Jumilla samples; Mg, Ni, Cr, Zr, Th, *LREE*, U, Pb, Ba, Sr and Rb are high (Rb may be relatively low at Jumilla); (iii) the $^{87}Sr/^{86}Sr$ value is unusually high

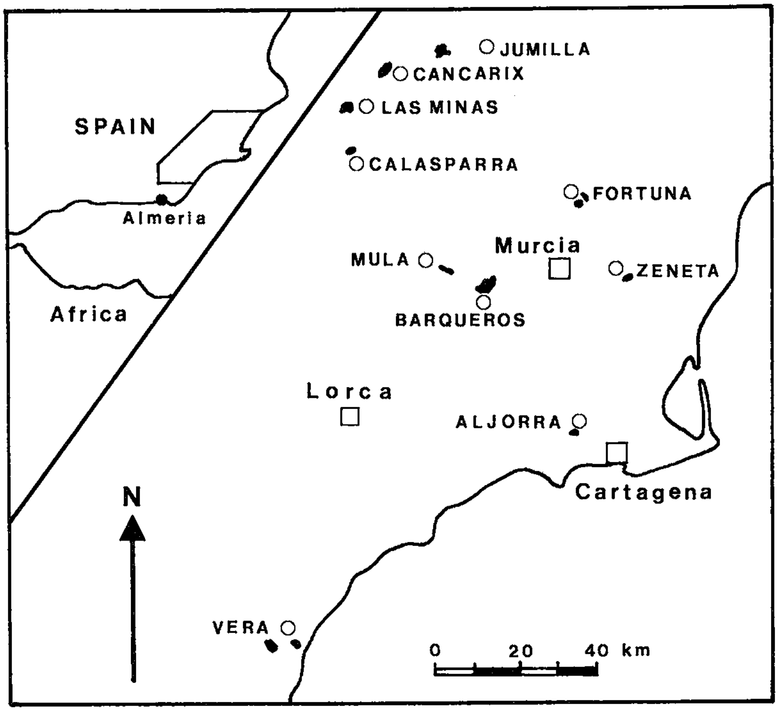

FIG. 1. Locations of the outcrops of lamproitic rocks in southeastern Spain.

(0.71750–0.72083), whereas the $^{143}Nd/^{144}Nd$ value is low (0.51119–0.51126); lead-isotope ratios are in the range $^{206}Pb/^{204}Pb$ 18.66–18.81, $^{207}Pb/^{204}Pb$ 15.67–15.74 and $^{208}Pb/^{204}Pb$ 39.0–30.2.

Detailed petrographic and geochemical investigations on the Spanish lamproitic rocks were reported in Fuster *et al.* (1967), Borley (1967), Fernandez & Hernandez Pacheco (1972), Lopez Ruiz & Rodriguez Badiola (1980), Venturelli *et al.* (1984), Nixon *et al.* (1984) and Nelson *et al.* (1986). Our main aim in this paper is to contribute to the knowledge of the crystallization history and genesis of these unusual rocks.

PETROGRAPHY AND MINERAL CHEMISTRY

The petrographic features of the Spanish rocks with lamproitic affinity are highly variable. All the rocks are porphyritic and some may be very rich in glass (Fortuna, Vera, Zeneta). Many rocks from Jumilla are holocrystalline and coarse grained. Olivine and phlogopite are present in variable proportions and are the most abundant mafic phases. Clinopyroxene may be abundant in some outcrops (Aljorra and Jumilla). The Spanish ultrapotassic rocks are the only lamproites containing magmatic orthopyroxene as a consequence of the high silica content. Magmatic orthopyroxene, with Mg# [100 $Mg/(Mg+Fe^{2+})$] ranging from 79–82, mainly occurs in several outcrops (*e.g.*, Aljorra, Cancarix, Fortuna) as microlites of the groundmass, and very rarely as reaction coronas mantling olivine. Biotite is an additional phase at Zeneta and Vera. Sanidine is the most abundant groundmass phase in the glass-poor or glass-free rocks. The glass of the groundmass is very rich in Si (64–71% SiO_2 on a dry basis). K-rich amphibole (3.0–4.5% K_2O, 5.0–6.3% CaO), very high in Ti (5.2–7.9% TiO_2) and very low in Al (0.0–1.7% Al_2O_3) crystallized later than sanidine in the groundmass. The amphibole is yellow to pinkish and some is mantled by green rims which are Ca-free and Fe-rich (19–21% FeO_{total}). Carbonates of presumed magmatic origin (Fuster *et al.* 1967, Pellicer 1973) occur at Aljorra, Jumilla and Vera. Sparse crystals of leucite occur in some samples from Jumilla and Vera (Fuster *et al.* 1967). Other phases are apatite, Cr-spinel, Fe-Ti-spinel and, sometimes, analcime, ilmenite and pseudobrookite.

Small ultramafic fragments and xenocrysts of mafic phases may be present. They include kinked olivine (Mg# 90–94), orthopyroxene (Mg# 90) and clinopyroxene (Mg# 90). Xenoliths/xenocrysts of crustal origin may also occur (mica schists and "granitic" fragments, quartz, K-feldspar, plagioclase, kyanite, andalusite, limestones).

TABLE 1. REPRESENTATIVE MICROPROBE DATA FOR OLIVINE, ORTHOPYROXENE AND CLINOPYROXENE

	Olivine					Orthopyroxene					Clinopyroxene			*		
	J	CL		J	CL	A	F	CX		F	A	F	CX	CL	J	F
	lr	lc	--r	x	x	s	sc	sc	--r	x	lr	s	s	s	s	x
SiO_2	40.50	40.69	40.00	40.47	40.40	54.25	54.32	55.00	55.00	55.75	54.78	53.00	53.45	54.60	53.10	52.00
TiO_2	-	-	-	-	-	0.60	0.61	0.46	0.21	-	0.48	0.86	0.84	0.94	0.80	0.29
Al_2O_3	-	-	-	-	-	1.38	0.80	0.04	-	4.05	0.07	0.46	0.32	0.33	0.56	2.67
Fe_2O_3	-	-	-	-	-	-	-	0.14	0.36	-	1.38	1.19	0.35	-	1.00	-
FeO	12.30	8.53	13.67	9.68	9.32	12.11	12.06	8.22	13.36	5.54	3.13	2.66	3.67	4.20	3.25	2.27
MnO	0.33	0.13	0.29	0.15	0.09	0.32	0.24	0.20	0.36	0.13	0.12	0.11	0.16	0.14	0.20	0.07
MgO	45.30	49.83	45.57	49.02	48.60	28.98	29.90	32.33	27.99	33.09	18.51	16.32	17.59	17.70	17.40	17.94
CaO	0.18	0.08	0.16	0.07	0.13	1.87	1.56	1.55	1.27	0.68	19.85	22.15	22.59	22.50	22.40	22.33
Na_2O	-	-	-	-	-	-	0.05	0.08	0.14	0.07	0.58	0.74	0.33	0.18	0.73	0.16
NiO	nd	0.38	0.18	0.29	nd	0.04	0.06	0.02	-	0.30	nd	0.07	nd	nd	nd	0.15
Cr_2O_3	nd	0.04	-	0.08	-	0.17	0.15	0.07	0.10	0.31	0.55	0.32	-	-	-	1.05
Total	98.61	99.68	99.87	99.76	98.54	99.72	99.75	98.11	98.79	99.92	99.45	97.88	99.30	100.59	99.44	98.93
Mg #	86.8	91.2	85.6	90.0	90.3	81.0	81.5	85.5	78.9	91.4	91.3	91.6	89.4	88.2	93.0	93.4

J Jumilla, CL Calasparra, A Aljorra, F Fortuna, CX Cancarix. Values expressed in weight %.

l, s = large, small crystal, x = xenocryst, c = core, r = rim, nd = not determined, Mg# = $100 \times Mg/(Mg+Fe^{2+})$

Fe_2O_3 for pyroxene has been calculated according to Cawthorn & Collerson (1974).

* after Venturelli et al.(1984).

A detailed description of the mineralogy is reported in the papers cited above. Here we confine ourselves to mineralogical data that will be used for petrogenetic interpretations, and also describe minerals that have not been described carefully in previous papers.

Olivine

Phenocrysts of olivine are widespread and have a magnesian core (Mg# *ca.* 87–91) and a magnesium-depleted rim (Mg# *ca.* 83–88; Table 1). The matrix olivine is usually enriched in iron. During the late stages of crystallization, some olivine was rimmed

TABLE 2. REPRESENTATIVE MICROPROBE DATA FOR PHLOGOPITE, AMPHIBOLE, SANIDINE AND APATITE

	Phlogopite							Amphibole				Sanidine		Apatite		
	F	J	CX		CL	Z	PM	J	CX	CM		J	CX	Z	J	PM
	lr	poik	lc	--r	lc	gm	l	s	s	sc	--r	l	s			
SiO_2	37.10	39.57	40.90	40.23	42.04	39.97	40.51	53.02	53.15	52.43	53.01	64.40	64.28	0.38	0.71	0.35
TiO_2	7.68	8.55	2.27	4.58	1.92	3.96	1.87	6.31	7.90	5.15	4.95	0.36	0.43	-	-	0.04
Al_2O_3	12.14	9.78	12.24	11.70	11.94	12.89	13.54	1.05	0.22	0.77	-	16.60	17.42	-	-	-
Fe_2O_3	2.03	1.56	0.67	1.13	0.60	1.94	0.87	-	-	-	-	3.06	1.40	-	-	-
FeO	7.78	5.95	2.56	4.34	2.31	7.44	3.35	5.92	6.93	4.50	18.96	-	-	0.37	0.12	0.26
MnO	0.09	0.10	0.07	0.02	0.04	0.04	0.02	0.10	0.10	0.11	0.60	-	-	-	-	0.09
MgO	16.49	19.33	23.88	21.89	24.74	19.19	23.12	18.19	15.42	18.90	7.57	0.15	0.08	0.51	0.27	0.47
CaO	-	-	-	-	-	-	-	5.53	5.33	6.28	-	0.07	-	53.53	52.63	53.93
Na_2O	0.36	0.30	0.16	0.09	0.18	0.36	0.14	5.39	4.86	4.93	7.51	1.81	0.48	-	-	-
K_2O	9.49	10.30	10.42	10.46	9.65	9.09	10.20	3.63	4.48	3.09	4.34	14.10	16.10	-	-	-
P_2O_5	nd	nd	nd	nd	nd	nd	nd	nd	nd	nd	nd	nd	nd	40.94	40.72	41.57
F	3.04	2.09	4.40	3.35	2.94	2.27	1.16	1.13	0.82	1.35	0.11	-	-	2.85	3.04	2.87
Cl	0.10	0.05	-	-	-	0.03	0.02	-	-	-	-	-	-	1.09	0.18	0.30
Total	96.30	97.58	97.57	97.87	96.36	97.18	94.80	99.27	99.21	97.51	97.05	100.55	100.19	99.67	97.72	99.82

F Fortuna, J Jumilla, CX Cancarix, CL Calasparra, Z Zeneta, PM Puebla de Mula, CM Las Minas de Hellin.

Fe_2O_3 for phlogopite has been calculated from FeO tot. considering $Fe_2O_3/FeO = 0.26$ (Fuster et al. 1967).

Where Fe_2O_3 is not reported, FeO = FeO tot. Values expressed in weight %.

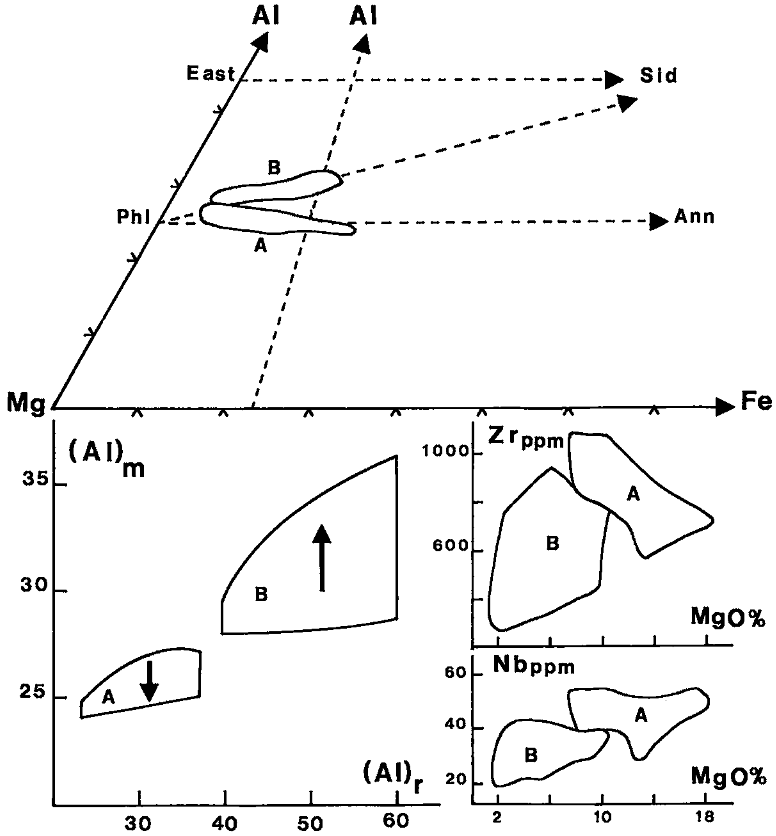

FIG. 2. Top part of the diagram shows the relation between phlogopite and host-rock chemistry. Group-A includes the outcrops of Jumilla, Cancarix, Las Minas de Hellin, Calasparra; group-B the outcrops of Vera, Aljorra, Zeneta, Fortuna, Puebla de Mula, Barqueros. At lower left, arrows in diagram $(Al)_m$-$(Al)_r$ indicate the pattern of zoning toward the rim and in the microcrysts. $(Al)_m$ and $(Al)_r$ represent the Al/(Al + Mg + Fe) ratio (atomic) in phlogopite and in the rock, respectively. At lower right, Zr, Nb, and MgO are bulk-rock contents. Data after Venturelli *et al.* (1984).

by orthopyroxene and phlogopite. Kinked xenocrysts (Mg# 90–94) occur in places. The uranium content of olivine has been determined by the fission-track method. The phenocrysts contain less uranium than xenocrysts (*e.g.*, 11–22 ppb and 58–115 ppb, respectively, for samples from Calasparra).

TABLE 3 . BEHAVIOR OF SOME ELEMENTS IN THE PHLOGOPITE

Mica group	ΔTi/Δ(Mg,Fe)	ΔTi/ΔAl	ΔTi/ΔSi	ΔAl/ΔSi
A	-0.97	-1.6	un	un
B	-0.99	un	-1.5	0.3 - 0.4

(a) $^{IV}Al + {}^{VI}Al + 3(Mg,Fe) = {}^{IV}Ti + 2{}^{VI}Ti + 2{}^{VI}\square$

un = no significant correlation

Brown mica

Phlogopite (Table 2), present as phenocrysts and microcrysts, commonly shows a Fe–Ti-enriched rim (FeO_{total} and TiO_2 up to 11.7 and 11.3%, respectively). Two main types of phlogopite may be recognized (Fig. 2). Group A (Jumilla, Cancarix, Calasparra, Las Minas de Hellin) exhibits a low Al/(Ca + Fe + Mg) atomic ratio and a trend subparallel to the phlogopite–annite join. Group B (Vera, Aljorra, Fortuna, Barqueros, Zeneta, Puebla de Mula) has higher Al/(Al + Fe + Mg) ratios and follows the phlogopite–siderophyllite join. The host rocks differ chemically (Fig. 2). The rocks with a lower Al/(Al + Fe + Mg) ratio contain mica of group A, whereas micas of group B occur in rocks with higher Al/(Al + Fe + Mg) ratio, suggesting that moderate variations in rock chemistry exert an important control on mica composition. In most cases the mica has (Si + Al) less than 4 and exhibits a correlation between Ti and (Mg + Fe) with a slope $\simeq 1$ (Δ Ti/Δ(Mg,Fe) $\simeq 1$). This trend differs from that usually found in mica from K-rich rocks (Arima & Edgar 1981). Considering Ti as tetravalent and disregarding the role of Fe^{3+}, the behavior of group-A micas may be explained through reaction (a) shown in Table 3; the behavior of group-B micas is more complicated and difficult to interpret.

All samples of mica investigated are rich in fluorine (1–4.4%), reflecting the high fluorine content of the host rocks (*ca.* 300–2600 ppm; R. Vannucci, pers. comm., 1983). High contents of fluorine in mica of lamproites and similar rocks have been reported by Cross (1897), Prider (1939), Jones & Smith (1983), Scott-Smith & Skinner (1984), Jaques (1986) and Foley *et al.* (1986b).

Oxides

Representative bulk compositions of the oxide minerals are shown in Table 4.

Spinel. Five different types of spinel have been identified (Fig. 3); more than one type may appear in the same sample: (i) Chromite (CHR, Cr_2O_3 in the range 39–63%) exhibits low to very low Al (0.9–3.4% Al_2O_3) and a Cr/Fe^{3+} ratio greater than 1.6. The chromite occurs mostly in olivine phenocrysts and may be considered as a near-liquidus phase. (ii) Cr magnetite (CrMT) has intermediate Cr, low to very low Al (sample 34 from Aljorra, Al_2O_3 5.83%, is an exception) and a Cr/Fe^{3+} ratio less than 1. (iii) Ti magnetite (TiMT) has very low Cr and

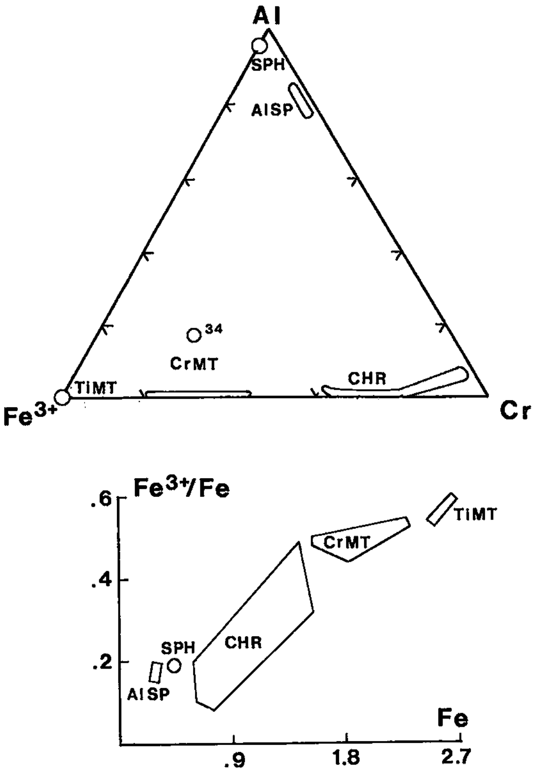

FIG. 3. Chemical features of the spinels (atoms in the formula on the basis of 4 atoms of oxygen and 3 cations). CHR: chromite, CrMT: Chromian magnetite, TiMT: Titanian magnetite, AlSP: Al-rich spinel, SPH: spinel-hercynite series. 34, sample from Aljorra.

TABLE 4. REPRESENTATIVE COMPOSITIONS OF OXIDE PHASES

	CHR				CrMT	AlSP	SPH	IL		MgPB	
	J	CX	CM	CL	J	F	J	J	CX	F	CM
	inOl	inOlr	inOl	inOl	gm	x		gm	gm	gm	gm
TiO_2	2.76	9.99	1.29	1.37	8.38	0.23	0.29	50.32	52.13	66.12	65.61
Al_2O_3	0.94	0.08	2.15	2.50	0.21	48.68	62.65	-	0.02	1.32	-
Cr_2O_3	39.09	32.31	63.62	63.35	10.65	18.24	-	0.10	0.77	0.33	0.19
Fe_2O_3	24.71	17.99	4.63	3.53	42.08	2.16	4.30	7.76	3.68	8.45	12.00
FeO	24.71	33.90	17.85	21.23	34.20	10.15	20.84	35.67	36.97	12.97	12.12
MnO	0.95	0.71	-	0.48	0.69	0.25	0.16	1.13	0.60	0.15	-
MgO	5.39	3.68	10.14	7.90	2.68	18.86	16.54	4.77	5.24	8.00	8.24
NiO	0.23	0.44	0.12	-	-	0.34	-	0.02	-	-	-
Total	98.78	99.10	99.80	100.36	98.89	98.91	100.95	99.77	99.41	97.34	98.16
Fe^{3+} #	36.8	34.6	6.2	4.8	78.5	2.2	4.2	98.7	82.0	77.8	98.3
Cr #	61.0	65.1	89.3	89.9	20.9	19.6	-	1.3	17.9	3.2	1.7

J Jumilla, CX Cancarix, CM Las Minas de Hellin, CL Calasparra, F Fortuna.

inOL in olivine, gm groundmass.

Fe^{3+} # = $100xFe^{3+}/(Al+Cr+Fe^{3+})$, Cr # = $100xCr/(Al+Cr+Fe^{3+})$, atomic ratios.

Fe_2O_3 calculated considering: total cations = 3 and valences = 8 for spinel, total cations = 2 and valences = 6 for ilmenite, total cations = 3 and valences = 10 for Mg-pseudobrookite.

CHR chromite, CrMT Cr-magnetite, AlSP Al-spinel, SPH spinel-hercynite series, IL ilmenite, MgPB Mg-pseudobrookite.

Al (<0.2% Cr_2O_3 and *ca.* 0.13% Al_2O_3). Along the sequence CHR→CrMT→TiMT, the Fe^{3+}/Fe ratio increases (Fig. 3). (iv) Al spinel (AlSP), very low in Ti (0.1–0.25% TiO_2), is either included in xenocrystic olivine or occurs as separate anhedral crystals; it is very similar to the spinel of lherzolite nodules common in alkali olivine basalts. (v) One category of spinel (SPH) belongs to the spinel–hercynite series; SPH is very poor in Cr (<0.15% Cr_2O_3), poor in Ti (*ca.* 0.3% TiO_2) and has a very low Fe^{3+}/Fe ratio, suggesting low $f(O_2)$ conditions. A similar type of spinel has been described in West Kimberley (Jaques & Foley 1985) and Leucite Hills lamproites (Kuehner *et al.* 1981). In the West Kimberley lamproite, SPH has been related to exsolution of nonstoichiometric leucite supersaturated in Mg, Al and Fe (Jaques & Foley 1985). In the Spanish rocks, spinel SPH has different features: (a) SPH may occur as tiny emerald-green grains contained in spongy brown mica (usually unstable biotite) along with sanidine(?) + ilmenite; spinel grains may be arranged in fine-grained aggregates mimicking the morphology of previous mica flakes. (b) SPH may constitute aggregates rimmed by phlogopite, generating characteristic snow-ball textures. Since the miscibility between $MgCr_2O_4$ and $MgAl_2O_4$ end members is complete (Muan *et al.* 1972), spinel of types (a) and (b) did not crystallize from the same melt that generated spinel CHR. Spinel of types (a) and (b) probably represent the product of the breakdown at different stages of a former unstable biotite that was richer in Fe and Al compared to the newly formed phlogopite.

A *pseudobrookite*-like mineral, identified in the groundmass of some samples, appears as small subhedral deep reddish grains with a low birefringence. In terms of the end members $MgTi_2O_5$, $FeTi_2O_5$ and Fe_2TiO_5, the composition is about 46, 37–42 and 12–17 mole%. The mineral is very similar to the Fe^{3+}-bearing armalcolite found by Velde (1975) in the Smoky Butte lamproites.

Clinopyroxene

Clinopyroxene commonly occurs as microcrysts and rarely as phenocrysts (Table 1). Approximate calculations of the end members (Cawthorn & Collerson 1974) suggest that the clinopyroxene is generally characterized by high Fe^{3+} content (up to 1.6% Fe_2O_3). The aluminum content is low, as is usual for low-Al ultrapotassic rocks. Xenocrystic pyroxene (Mg# 90) is encountered only rarely.

Sanidine

Sanidine (Table 2) is present in the groundmass; in some coarse-grained rocks from Jumilla it may constitute large poikilitic crystals. It may have high contents of Fe^{3+} (up to 3.5% Fe_2O_3), Ti (up to 0.43% TiO_2) and Ba (up to 1.9% BaO, Venturelli *et al.* 1984).

Apatite

Apatite is always present and is locally abundant as euhedral crystals (Jumilla, Puebla de Mula). It is very rich in fluorine (Table 2).

EVALUATION OF TEMPERATURE OF EQUILIBRATION

Olivine–melt equilibrium has been tested in the Calasparra samples in which (i) olivine is the only large phenocryst present and (ii) its weight proportion may be correctly evaluated (*ca.* 20% wt.). To test for equilibrium and to determine the temperature of crystallization, we used equation (3) of Ford *et al.* (1983) and equation (17) of Ghiorso *et al.* (1983). The former is an empirical equation that considers the influence of composition and structure of the melt on the component activities; the latter uses an iterative calculation taking into account the mineral–liquid equilibrium constant and the activities of the liquid and mineral components. Both equations, however, call for Fe_2O_3 concentrations in the melt. Since chromite crystallized contemporaneously with the olivine phenocrysts at Calasparra, the Fe^{3+}/Fe^{2+} ratio of the melt has been calculated using the $K_{DSP/L}^{Fe^{2+}-Fe^{3+}}$ value obtained by Foley (1985) for the Gaussberg lamproite, which has a chemistry very similar to that of the Spanish ultrapotassic rocks and contains comparable Cr-rich spinel (Sheraton & Cundari 1980, Foley 1985). The temperature of crystallization of olivine so obtained (*ca.* 1200°C), is not far from that obtained during the experiments on Gaussberg material (1270°C; Foley 1985) with no volatile present. The calculated temperature of olivine crystallization must be considered with caution because the Spanish lamproitic magmas contained volatiles (mainly H_2O) and had an unusual composition (low Na and Al, and high K). The temperature represents an upper limit because water depresses the temperature of crystallization.

In the coarse-grained subvolcanic rocks of Jumilla, where ilmenite and magnetite occur as late phases, the temperature has been estimated using a Buddington & Lindsley type of geothermometer (Stormer 1983, pers. comm., Spencer & Lindsley 1981). As both ilmenite and magnetite are homogeneous, the low values obtained (740–820°C) are considered as late-magmatic temperatures.

Fluorine and hydroxyl distribution between apatite and coexisting mica is a potential geothermometer. Stormer & Carmichael (1971) obtained an approximate temperature–composition relation using fluorides and magnesium and calcium hydroxides.

More recently Chernysheva *et al.* (1976) and Ludington (1978) obtained more reliable equations for the equilibria:

biotite(OH) + HF = biotite(F) + H_2O (1)

apatite(OH) + HF = apatite(F) + H_2O (2)

apatite(OH) + biotite(F) = apatite(F) + biotite(OH) (3)

Using different data relative to reaction (2) and assuming the mica to be phlogopite, Chernysheva *et al.* (1976) and Ludington (1978) obtained equations for the dependence of log$K$(3) on the reciprocal of absolute temperature [(1324/T)-0.16 and 1100/T, respectively]. Using the equation reported by Ludington & Munoz (1975), temperature may be corrected for the influence of mica components other than phlogopite. The temperature evaluation is only approximate because of (i) the heterogeneous distribution of F in mica and (ii) the difficulty in calculating correctly the mole fractions of OH and F and of the phlogopite, annite and siderophyllite components in the mica. The low values obtained (580-730°C) suggest that F$\rightleftharpoons$OH exchange between apatite and mica continued to temperatures below the solidus.

TEMPERATURE-OXYGEN FUGACITY PATHS

The state of oxidation of the iron in the silicate melts depends on $f(O_2)$, temperature, pressure, and composition (structure) of the liquid. Assuming the other parameters to be constant, the Fe^{3+}/Fe^{2+} ratio increases with decreasing temperature (Sack *et al.* 1980, Kilinc *et al.* 1983, and references therein) and decreasing pressure (Mysen & Virgo 1978). The relationship between Fe^{3+}/Fe^{2+} and composition has been discussed by Douglas *et al.* (1965), who considered a redox reaction of the type:

$$Fe^{2+} + \tfrac{1}{4} O_2 = Fe^{3+} + \tfrac{1}{2} O^{2-}. \qquad (4)$$

These authors found that $K(4)$ depends largely on composition. Fe^{3+}/Fe^{2+} ratio, oxygen-ion activity and $K(4)$ increase with the basicity of the melt; however, it is not possible to evaluate separately the role of the individual parameters. More recently, Virgo *et al.* (1981) found that the composition of melts and their degree of polymerization influence the Fe^{3+}/Fe^{2+} ratio. Sack *et al.* (1980) and Kilinc *et al.* (1983) have proposed empirical equations linking Fe^{3+}/Fe^{2+}, temperature, composition of the silicate melts and $f(O_2)$. These empirical equations are poorly calibrated for alkalis (alkaline rocks form only a small part of the database) and yet the com-

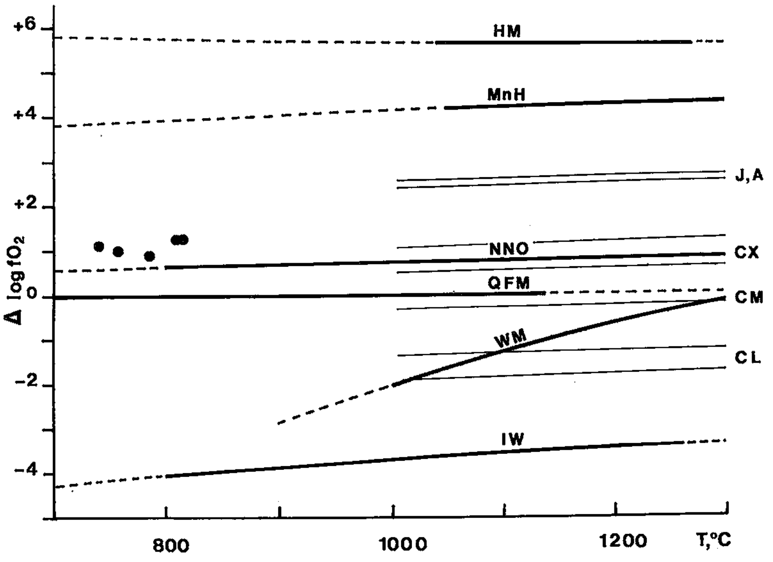

FIG. 4. Paths of oxygen fugacity *versus* temperature for some rocks investigated. J Jumilla, A Aljorra, CX Cancarix, CM Las Minas de Hellin, CL Calasparra. The equations for the buffers HM, QFM, WM, IW are after Myers & Eugster (1983), and for MnH ($Mn_{1-x}O$ - Mn_3O_4) and NNO after Huebner & Sato (1970). $\Delta \log f(O_2) = \log f(O_2)$ (sample)-$\log f(O_2)$ (QFM). Thin lines = rocks, thick lines = buffers. Filled circles refer to data obtained for the coarse-grained rocks of Jumilla using magnetite-ilmenite pairs.

positional terms for alkalis are very significant. It is encouraging to note, however, that there is a good agreement between the data obtained using such equations and wet-chemical measurements of Fe^{3+}/Fe^{2+} ratio in experimental products obtained in a lamproitic system (Foley 1985).

Because the Fe^{3+}/Fe^{2+} values of the melt and of the crystallizing phases are related in some way, the value in the phases will also depend on the liquid composition. This, of course, places limits on the use of the geothermometer–geobarometer proposed by Buddington & Lindsley (1964). Moreover, the ilmenite–magnetite pair is found only rarely in these lamproitic rocks. Consequently, we relied mainly on the empirical equation proposed by Kilinc *et al.* (1983) to determine potential temperature-$f(O_2)$ paths for the rocks investigated.

The Fe^{3+}/Fe^{2+} ratio of the melt may be calculated approximately using the value of $K_{DSP/L}^{Fe^{2+}-Fe^{3+}}$ reported by Foley (1985) and the data for Cr spinel in the Spanish rocks. Consequently, $f(O_2)$ may be calculated at constant Fe^{3+}/Fe^{2+} ratio for different temperatures using the empirical equation proposed by Kilinc *et al.* (1983):

$$\ln[X(Fe_2O_3)/X(FeO)] = a \ln f(O_2) + b/T + c + \Sigma diXi \qquad (5)$$

where *a*, *b* and *c* are constants, *d* are constants for different oxide components in the melt from which the Cr spinel crystallizes, and *X* are the mole fractions. The temperature-$f(O_2)$ paths obtained are reported in Figure 4. Samples from Calasparra exhibit the lowest $f(O_2)$ trend (close to the MW buffer) and the rocks from Aljorra and Jumilla, the highest $f(O_2)$. The redox conditions of the Las Minas de Hellin, Cancarix and Fortuna materials are similar to those of West Kimberley and Gaussberg lamproite (Foley 1985). The temperature-$f(O_2)$ paths reported are strictly correct only if the following assumptions are fulfilled: (i) the distribution coefficient for Cr spinel is not significantly dependent on temperature in the range 1000–1300°C; (ii) the redox state of Cr spinel in olivine did not change significantly after crystallization; and (iii) extrapolation of equation (5) from FMQ to MW conditions does not induce serious errors.

The rocks from Jumilla are the only samples containing Ti magnetite (besides Cr spinel) and ilmenite, which crystallized during the intermediate to late stages under subvolcanic conditions. The temperature-$f(O_2)$ pattern obtained using a Buddington & Lindsley type of geothermometer–geobarometer (Stormer 1983, pers. comm., Spencer & Lindsley 1981), is reported in Figure 4; $f(O_2)$ is in the range $10^{-14.8}$ to $10^{-12.9}$ atm.

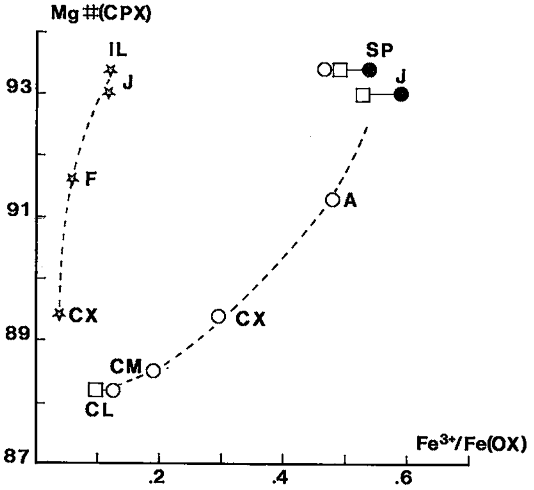

FIG. 5. Mg# [$=Mg \times 100/(Mg+Fe^{2+})$] for clinopyroxene *versus* Fe^{3+}/Fe ratio in spinel and ilmenite. Symbols as in Figure 4 with the addition of F Fortuna; SP spinel; IL ilmenite; open circle: Cr-spinel in olivine; square: Cr spinel not included in olivine; filled circle: titanian magnetite.

TABLE 5. REPRESENTATIVE DATA ON MICA AND APATITE AND ON HF, HCl, H_2O FUGACITY RATIOS

Localities	Jumilla		Puebla de Mula	
Mica(1)	(i)	(ii)	(i)	(ii)
X(F)	0.240	0.240	0.132	0.132
X(OH)	0.758	0.716	0.866	0.843
X(Phl)	0.764	0.764	0.732	0.730
X(Ann)	0.103	0.132	0.073	0.060
X(Sid+East)	-	-	0.159	0.159
$\log(fHF/fH_2O)$	-4.1	-4.1	-4.0	-4.0
Apatite(2)				
X(F)	0.875		0.753	
X(Cl)	0.021		0.043	
X(OH)	0.104		0.204	
$\log(fHF/fH_2O)$	-4.8	-4.9	-4.0	-4.0
$\log(fHCl/fH_2O)$	-4.3	-4.3	-3.8	-4.0
Apatite/mica				
T,°C	611	605	751	749

Fugacity ratios calculated (1) according to Ludington & Munoz (1975) and (2) according to Korzhinskiy (1981). Temperatures calculated according to Ludington (1978). X = mole fraction. The mole fractions have been calculated in the following way:

a. Mica. (i) On the basis of a formula where all iron as been considered as divalent, valences = 22 and (F+ +Cl+OH) = 2. (ii) Fe^{3+}= 0.187 Fe tot. (i.e., Fe_2O_3/FeO= =0.26,cf.,Fuster et al. 1967) and OH = (2-F-Cl-O) where O = Fe^{3+}.

b. Apatite. On the basis of (F+Cl+OH) = 1.

RELATIONS BETWEEN OXIDES AND SILICATE PHASES

Comparable oxygen fugacity – temperature paths were obtained using Cr spinel included in olivine, and Cr spinel occurring as isolated crystals; the results suggest that the spinels are of same generation and that their Fe^{3+}/Fe^{2+} ratio was not influenced greatly by olivine–spinel subsolidus reequilibration. The Fo content of olivine does not increase with $f(O_2)$ in the rocks investigated; instead, it decreases roughly with an increasing Fe^{3+}/Fe^{2+} ratio in the coexisting Cr spinel. This suggests that temperature and melt composition were probably more important in controlling the Fo content of olivine than $f(O_2)$. In contrast, the composition of clinopyroxene, which began to crystallize later than olivine, was strongly influenced by the value of $f(O_2)$, as suggested by the good correlation between its Mg# and the Fe^{3+}/Fe^{2+} ratio of the spinel (Fig. 5) This correlation also suggests (i) that the composition of the Cr spinel reflects the redox conditions when clinopyroxene crystallized, and (ii) that the oxidation state of the Cr spinel did not change significantly during the latest stages of crystallization and at subsolidus conditions.

ACTIVITIES OF VOLATILE COMPONENTS

The $f(HF)/f(H_2O)$ and $f(HCl)/f(H_2O)$ ratios may be calculated from $HF \rightleftharpoons H_2O$ and $HCl \rightleftharpoons H_2O$ exchange equilibria involving mica and apatite. Ludington & Munoz (1975) and Korzhinskiy (1981) reported useful equations determined experimentally assuming ideal solution between the components of the solid phase and ideal mixing of the components in the gas phase. The data obtained (Table 5) are approximate for the same reasons we have pointed out in the section concerning the temperature evaluation. In spite of the high content of fluorine in biotite and apatite, the fugacity ratios obtained suggest that H_2O was dominant over HF.

That CO_2 also played some role during petrogenesis is suggested by the presence of magmatic carbonates (Fuster *et al.* 1967, Pellicer 1973). The carbonates may be related to CO_2 incorporated from country rocks (*e.g.*, limestones) after magma segregation, or to authigenic CO_2. In the latter case, since the high-SiO_2 Spanish lamproitic magmas cannot have been generated in a CO_2-rich source, CO_2 could be due to oxidation, during emplacement and crystallization, of CH_4 present in a reduced source (*cf.* Foley *et al.* 1986b).

FEATURES OF THE MANTLE SOURCE AND THE ORIGIN OF THE MELTS

Nelson *et al.* (1986) used lead isotope data and Foley *et al.* (1987) used mainly chemical features to infer a depleted mantle source for the Spanish magmas. However, the high content of "incompatible" elements suggests enrichment of the early-depleted mantle source. Sr, Nd and Pb isotopes are in agreement with a metasomatic component that had the "characteristics of continental crust or sediments derived from the continental crust" (Nelson *et al.* 1986, p. 239). Furthermore, the unusually high content of uranium in the olivine xenocrysts also supports mantle metasomatism. The high to very high K/Na ratio and low Na values, and the high P content, suggest that phlogopite and apatite were involved during the mantle melting.

That the distribution of trace and some major elements in the most magnesian (MgO > 9%) Spanish lamproites gives no evidence of fractionation from a single magma is suggested by the following: (i) Mg is not correlated with many "incompatible" elements (*e.g.*, Zr, Nb, Rb); (ii) taking into account that olivine is usually the first major mineral which crystallized during the emplacement of the magmas, the variation of the Ni content (670–380 ppm) in the fine- to medium-grained rocks is too low if compared with the olivine fractionation required (*ca.* 20%) to explain the large variation in Mg (*ca.* 13–9% MgO) (Venturelli *et al.* 1984); (iii) the $^{87}Sr/^{86}Sr$ ratio is largely variable (Nelson *et al.* 1986).

The high Ni (> 380 ppm) and Cr (> 610 ppm) contents and the high Mg# (67–78) in the most magnesian rocks (MgO > 9%) suggest that they could be regarded as near-primary, mantle-derived magmas.

In a previous study of Spanish lamproites (Venturelli *et al.* 1984), a potential loss of Na as NaF during crystallization was suggested. Owing to the high capacity of the alkaline melts to dissolve volatile components, the NaF loss could have been significant only if F was very abundant in the magmas. This is not supported by any geological and petrographic evidence as, for instance, the presence of products of interaction between F-rich fluids and the country rocks. Thus we believe that at least the composition of the fine- to medium-grained rocks is not far from that of the melts before crystallization and near-surface emplacement.

The data of Luth (1967) and unpublished data of A.K. Gupta and D.H. Green, quoted by Foley *et al.* (1986a), for the system Ks–Fo–Qtz (Fig. 6), suggest that the PHL + EN + FO + L peritectic point moves toward lower Fo/Ks values and higher Qtz content as pressure decreases (Fig. 6, top), whereas the F/H_2O ratio affects the position of the peritectic in a direction transverse to the pressure trend. A shift of the EN + FO + L peritectic line away from Qtz with increasing pressure is also seen in the dry experiments of Kushiro (1980).

Let us consider a source consisting of a phlogopite-bearing peridotite with a composition falling in the

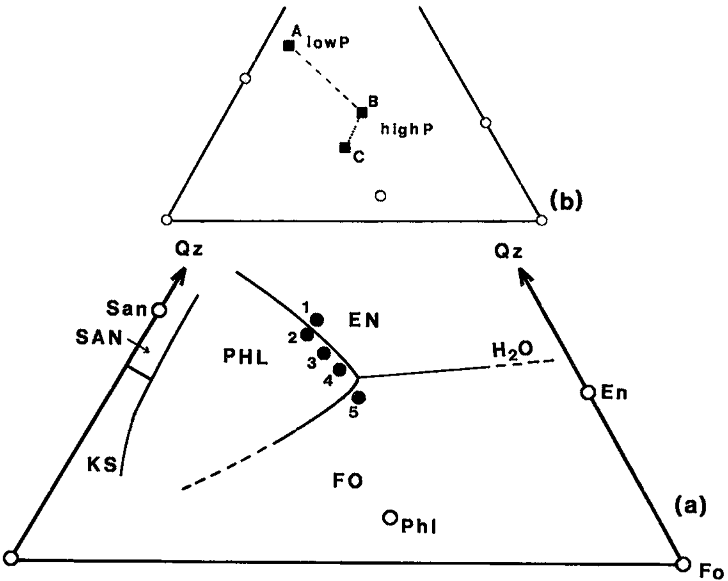

FIG. 6. *a*. Qtz(silica)–Ks(kalsilite)–Fo(olivine) diagram for the investigated rocks with MgO >9%. (1) Fortuna, (2) Las Minas de Hellin (3) Cancarix, (4) Calasparra, (5) Jumilla (fine-grained rocks). The coarse-grained rocks from Jumilla have been omitted because the K/Na ratio may have been significantly modified by late crystallization of analcime. Normative data are average values obtained from chemical analyses reported by Venturelli *et al.* (1984). Phase fields (capital letters) for water-rich and for volatile-free system at 28 kbar are after Foley *et al.* (1986a, b), based on unpublished data of A.K. Gupta & D.H. Green. *b*. Point A and point B represent the PHL + FO + EN + L peritectic point at 3 kbar (Luth 1967) and 28 kbar (A.K. Gupta & D.H. Green, unpubl.), respectively, for a water-rich system. C is the peritectic point for a F-bearing water-free system at 28 kbar (Foley *et al.* 1986a). Thus, as pressure decreases, the peritectic point moves away from the Fo corner, whereas the variation of the F/H_2O ratio changes the position of the peritectic point in a direction transverse to the trend for increasing pressure.

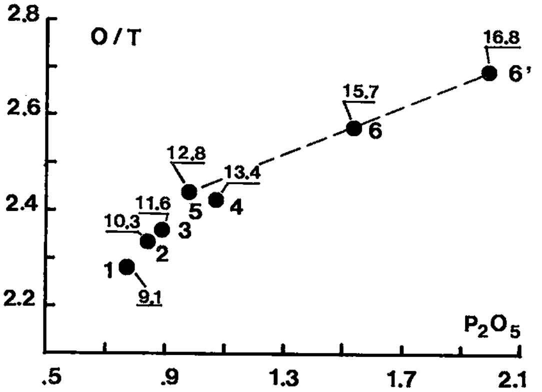

FIG. 7. O/T ratios *versus* P_2O_5 contents for the investigated rocks with MgO >9%. Symbols of the localities are as in Figure 6. MgO contents (underlined) are also reported for the different outcrops. O/T = oxygen/(Si + Ti + Al + Fe^{3+}) atomic ratio calculated assuming a dry basis and Fe_2O_3/FeO = 0.32, a value found in the most fresh rocks. Data after Venturelli *et al.* (1984). The tie-line connects the samples from Jumilla (6 and 6′ are coarse-grained rocks).

triangle Phl–En–Fo (Fig. 6). The compositions of the rocks from Fortuna (1), Las Minas de Hellin (2), Cancarix (3), Calasparra (4) and Jumilla (5, fine-grained rocks) may correspond to peritectic melts generated from such a source under hydrated conditions at different depths. Assuming that fractional crystallization was not significant, the Spanish magmas could have been generated at pressures lower than 30 kbar.

If we assume that the source did not contain abundant phlogopite, the amounts of liquid formed near the peritectic point would represent a low to moderate degree of partial melting. Thus the low contents of Sc (13–15 ppm), Na (0.64–1.9% Na_2O), Al (8–11.8% Al_2O_3) and Ca (2.6–4.9% CaO) would reflect a source which, before the enrichment in "incompatible" elements, underwent a strong depletion (loss of clinopyroxene and garnet).

If, as an alternative, we assume that the source was composed mainly of phlogopite and orthopyroxene, and lower amounts of olivine and clinopyroxene, the proportion of melt may be very high; the low contents of Sc, Na, Al and Ca may reflect a dilution effect rather than a strongly depleted nature of the source. A source very rich in phlogopite may be unusual, but is possible. The rarity of such a source would be consistent with the scarcity of lamproitic rocks world-wide. It is unlikely, however, that high proportions of melt can exist in the mantle without moving off (McKenzie 1984). The proposal of a high degree of melting, therefore, would require fractional melting followed by coalescence of the batches of melt.

For the outcrops investigated, the O/T ratio (oxygen/tetrahedral sites) and the MgO contents are well correlated with P_2O_5 (Fig. 7), suggesting that apatite solubility decreases with increasing degree of polymerization and with decreasing temperature, in agreement with experimental data (Kogarko *et al.* 1981). The trend (1)-(2)-(3)-(4)-(5) (Fig. 7) suggests that apatite was a potential residual phase, or that it only just melted during partial melting of the source.

Granted that the melts were saturated in P_2O_5 and that apatite in the mantle dissolves easily into the melts, the second melting hypothesis reported above requires a large amount of apatite at the source. The scattered distribution of Zr, Nb, Ce and Th in the rocks may be explained by melting of a source that had a heterogeneous distribution of accessory minerals.

The Jumilla outcrop is a petrological oddity. The rocks are mainly coarse-grained and exhibit unusual chemical features: the MgO content and the O/T ratio correlate positively not only with P_2O_5 (Fig. 7) but also with Zr, Nb, Ce and Th (Venturelli *et al.* 1984). This may be explained in two different ways: (i) the rocks formed from a magma produced by prograde partial melting of a source containing residual minor and accessory minerals (apatite included); (ii) the trend was generated by processes of fractional crystallization and accumulation involving not only olivine, but also phases containing the high-valency elements listed before. For these accessory phases, petrographic evidence suggests that only apatite formed large crystals during crystallization. Moreover, the observed variation of Ni content (from 740 to 670 ppm) suggests that significant fractionation of olivine has not occurred.

ACKNOWLEDGEMENTS

We are grateful to the referees for their useful suggestions and to Dr. R.F. Martin for his careful review of the manuscript. Financial support was from Ministero della Pubblica Istruzione, Rome (grant n. 021202-051320, 40% M.P.I.).

REFERENCES

ARIMA, A. & EDGAR, A.D. (1981): Substitution mechanism and solubility of titanium in phlogopites from rocks of probable mantle origin. *Contr. Mineral. Petrology* **77**, 288-295.

BELLON, H., BORDET, P. & MONTENAT, C. (1983): Chronologie du magmatisme Néogène des Cordillères Bétiques (Espagne Méridionale). *Bull. Soc. Géol. France* **25**, 205-217.

BORLEY, G.D. (1967): Potash-rich volcanic rocks from southern Spain. *Mineral. Mag.* **36**, 364-379.

BUDDINGTON, A.F. & LINDSLEY, D.H. (1964): Iron-titanium oxide minerals and synthetic equivalents. *J. Petrology* **5**, 310-357.

CAWTHORN, R.G. & COLLERSON, K.D. (1974): The recalculation of pyroxene end-member parameters and the estimation of ferrous and ferric iron content from electron microprobe analyses. *Amer. Mineral.* **59**, 1203-1208.

CHERNYSHEVA, YE.A., PETROV, L.L. & CHERNYSHEV, L.V. (1976): Distribution of fluorine between coexisting phlogopite and apatite in carbonatites and the behaviour of fluorine in the carbonatite-forming processes. *Geochem. Int.* **13**, 14-22.

CROSS, W. (1897): Igneous rocks of the Leucite Hills and Pilot Butte, Wyoming. *Amer. J. Sci.* **4**, 115-141.

DOUGLAS, R.W., NATH, P. & PAUL, A. (1965): Oxygen ion activity and its influence on the redox equilibrium in glasses. *Phys. Chem. Glasses* **6**, 216-223.

FERNANDEZ, S. & HERNANDEZ PACHECO, A. (1972): Las rocas lamproiticas de Cabezo Negro, Zeneta (Murcia). *Estudios Geol. (Madrid)* **28**, 267-276.

FOLEY, S.F. (1985): The oxidation state of lamproitic magmas. *Tschermaks Mineral. Petrog. Mitt.* **34**, 217-238.

______, TAYLOR, W.R. & GREEN, D.H. (1986a): The effect of fluorine on phase relationships in the system $KAlSiO_4$-Mg_2SiO_4-SiO_2 at 28 kbar and the solution mechanism of fluorine in silicate melts. *Contr. Mineral. Petrology* **93**, 46-55.

______, ______ & ______ (1986b): The role of fluorine and oxygen fugacity in the genesis of the ultrapotassic rocks. *Contr. Mineral. Petrology* **94**, 183-192.

______, VENTURELLI, G., GREEN, D.H. & TOSCANI, L. (1987): The ultrapotassic rocks: characteristics, classification, and constraints for petrogenetic models. *Earth Sci. Rev.* **24**, 81-134.

FORD, C.E., RUSSELL, D.G., CRAVEN, J.A. & FISK, M.R. (1983): Olivine-liquid equilibria: temperature, pressure and composition dependence of the crystal/liquid cation partition coefficients for Mg, Fe, Ca and Mn. *J. Petrology* **24**, 256-265.

Fuster, J.M., Gastesi, P., Sagredo, J. & Fermoso, M.L. (1967): Las rocas lamproiticas de SE de España. *Estudios Geol. (Madrid)* **23**, 35-69.

Ghiorso, M.S., Carmichael, I.S.E., Rivers, M.L. & Sack, R.O. (1983): The Gibbs free energy of natural silicate liquids; an expanded regular solution approximation for the calculation of magmatic intensive variables. *Contr. Mineral. Petrology* **84**, 107-145.

Huebner, J.S. & Sato, M. (1970): The oxygen fugacity–temperature relationships of manganese oxide and nickel oxide buffers. *Amer. Mineral.* **55**, 934-952.

Jaques, A.L. (1986): F-rich micas in the West Kimberley lamproites; contrasts with kimberlites and other micaceous alkaline ultramafic intrusions. *Fourth Int. Kimberlite Conf. Geol. Soc. Australia* **16**, 45-47 (abstr.).

______ & Foley, S.F. (1985): The origin of Al-rich spinel inclusions in leucite from the leucite lamproites of Western Australia. *Amer. Mineral.* **70**, 1143-1150.

Jones, A.P. & Smith, J.V. (1983): Petrological significance of mineral chemistry in the Agathla Peak and the Thumb minettes, Navajo volvanic field. *J. Geol.* **91**, 643-656.

Kilinc, A., Carmichael, I.S.E., Rivers, M.L. & Sack, R.O. (1983): The ferric–ferrous ratio of natural silicate liquids equilibrated in air. *Contr. Mineral. Petrology* **83**, 136-140.

Kogarko, L.N., Petrova, E.N. & Venturelli, G. (1981): Phosphate content of magmatic melts. *Dokl. Akad. Nauk SSSR* **261**, 1430-1432.

Korzhinskiy, M.A. (1981): Apatite solid solsutions as indicators of the fugacity of HCl and HF in hydrothermal fluids. *Geochem. Int.* **18**, 44-60.

Kuehner, S.M., Edgar, A.D. & Arima, M. (1981): Petrogenesis of the ultrapotassic rocks from the Leucite Hills, Wyoming. *Amer. Mineral.* **66**, 663-677.

Kushiro, I. (1980): Changes with pressure of degree of partial melting and K_2O content of liquids in the system Mg_2SiO_4–$KAlSiO_4$–SiO_2. *Carnegie Inst. Wash. Year Book* **79**, 267-271.

Lopez Ruiz, J. & Rodriguez Badiola, E. (1980): La region volcanica Neogena del sureste de España. *Estudios Geol. (Madrid)* **36**, 5-63.

Ludington, S.D. (1978): The biotite–apatite geothermometer revisited. *Amer. Mineral.* **63**, 551-553.

______ & Munoz, J.L. (1975): Application of fluorhydroxyl exchange data to natural micas. *Geol. Soc. Amer. Abstr. Programs* **7**, 1179.

Luth, W.C. (1967): Studies in the system $KAlSiO_4$–Mg_2SiO_4–SiO_2–H_2O: I, Inferred phase relations and petrological applications. *J. Petrology* **8**, 372-416.

McKenzie, D. (1984): The generation and compaction of partially molten rock. *J. Petrology* **25**, 713-765.

Muan, A., Hauck, J. & Lofall, T. (1972): Equilibrium studies with a bearing on lunar rocks. *Proc. third Lunar Sci. Conf.*, 185-196.

Myers, J. & Eugster, H.P. (1983): The system Fe–Si–O: oxygen buffer calibration to 1,500 K. *Contr. Mineral. Petrology* **82**, 75-90.

Mysen, B.O. & Virgo, D. (1978): Influence of pressure, temperature and bulk composition on melt structures in the system $NaAlSi_3O_8$–$NaFe^{3+}Si_2O_6$. *Amer. J. Sci.* **278**, 1307-1322.

Nelson, D.R., McCulloch, M.T. & Sun, S.-S. (1986): Origins of ultrapotassic rocks as inferred from Sr, Nd and Pb isotopes. *Geochim. Cosmochim. Acta* **50**, 231-245.

Nixon, P.H., Thirlwall, M.F., Buckley, F. & Davis, C.J. (1984): Spanish and Western Australian lamproites: aspects of whole rock geochemistry. *In* Kimberlites. I: Kimberlites and Related Rocks. Elsevier, Amsterdam.

Nobel, F.A., Andriessen, P.A.M., Hebeda, E.H., Priem, H.N.A. & Rondeel, H.E. (1981): Isotopic dating of the post-Alpine Neogene volcanism in the Betic Cordilleras, southern Spain. *Geol. Mijnbouw* **60**, 209-214.

Pellicer, M.J. (1973): Estudio petrologico y geoquimico de un nuevo yacimiento de rocas lamproiticas situado en las proximidades de Aljorra (Murcia). *Estudios Geol. (Madrid)* **29**, 99-106.

Prider, R.T. (1939): Some minerals from the leucite-rich rocks of the Western Kimberley area, Western Australia. *Mineral. Mag.* **25**, 273-387.

Puga, E. (1980): Hypothèse sur le genèse des magmatismes calcoalcalins, intra-orogénique et postorogénique alpins, dans les Cordillères Bétiques. *Bull. Soc. Geol. France* **22**, 243-250.

Sack, R.O., Carmichael, I.S.E., Rivers, M. & Ghiorso, M.S. (1980): Ferric-ferrous equilibria in natural silicate liquids at 1 bar. *Contr. Mineral. Petrology* **75**, 369-376.

Scott-Smith, B.H. & Skinner, E.M.W. (1984): A new look at Prairie Creek, Arkansas. *In* Kimberlites. I: Kimberlites and related rocks. Elsevier, Amsterdam.

SHERATON, J.W. & CUNDARI, A. (1980): Leucites from Gaussberg, Antarctica. *Contr. Mineral. Petrology* **71**, 417-427.

SPENCER, K.J. & LINDSLEY, D.A. (1981): A solution model for coexisting iron–titanium oxides. *Amer. Mineral.* **66**, 1189-1201.

STORMER, J.C. (1983): The effects of recalculation on estimates of temperature and oxygen fugacity from analyses of multicomponent iron–titanium oxides. *Amer. Mineral.* **68**, 586-594.

______ & CARMICHAEL, I.S.E. (1971): Fluorine–hydroxyl exchange in apatite and biotite: a potential igneous geothermometer. *Contr. Mineral. Petrology* **31**, 121-131.

VELDE, D. (1975): Armalcolite–Ti-phlogopite–diopside–analcite-bearing lamproites from Smoky Butte, Garfield County, Montana. *Amer. Mineral.* **60**, 566-573.

VENTURELLI, G., CAPEDRI, S., DI BATTISTINI, G., CRAWFORD, A., KOGARKO, L.N. & CELESTINI, S. (1984): The ultrapotassic rocks from southeastern Spain. *Lithos* **17**, 37-54.

VIRGO, D., MYSEN, B.O. & SEIFERT, F. (1981): Relationship between the oxidation state of iron and the structure of the silicate melts. *Carnegie Inst. Wash. Year Book* **80**, 308-310.

Received January 6, 1987; revised manuscript accepted March 27, 1987.